



HAL
open science

Group Theory of Messenger RNA Metabolism and Disease

Michel Planat, Marcelo M Amaral, David Chester, Fang Fang, Raymond Aschheim, Klee Irwin

► **To cite this version:**

Michel Planat, Marcelo M Amaral, David Chester, Fang Fang, Raymond Aschheim, et al.. Group Theory of Messenger RNA Metabolism and Disease. *Gene Expression: International Journal of Molecular and Cellular Science*, 2024, 23 (4), pp.264 - 272. 10.14218/GE.2023.00079 . hal-04723354

HAL Id: hal-04723354

<https://hal.science/hal-04723354v1>

Submitted on 7 Oct 2024

HAL is a multi-disciplinary open access archive for the deposit and dissemination of scientific research documents, whether they are published or not. The documents may come from teaching and research institutions in France or abroad, or from public or private research centers.

L'archive ouverte pluridisciplinaire **HAL**, est destinée au dépôt et à la diffusion de documents scientifiques de niveau recherche, publiés ou non, émanant des établissements d'enseignement et de recherche français ou étrangers, des laboratoires publics ou privés.

GROUP THEORY OF MESSENGER RNA METABOLISM AND DISEASE

MICHEL PLANAT[†], MARCELO AMARAL[‡], DAVID CHESTER[‡], FANG FANG[‡]
RAYMOND ASCHHEIM[‡] AND KLEE IRWIN[‡]

ABSTRACT. Our recent work has focused on the application of infinite group theory and related algebraic geometric tools in the context of transcription factors and microRNAs. We were able to differentiate between “healthy” nucleotide sequences and disrupted sequences that may be associated with various diseases. In this paper, we extend our efforts to the study of messenger RNA metabolism, showcasing the power of our approach. We investigate (i) mRNA translation in prokaryotes and eukaryotes, (ii) polyadenylation in eukaryotes, which is crucial for nuclear export, translation, stability, and splicing of mRNA, (iii) miRNAs involved in RNA silencing and post-transcriptional regulation of gene expression, and (iv) the identification of disrupted sequences that could lead to potential illnesses. To achieve this, we employ (a) infinite (finitely generated) groups f_p , with generators representing the $r + 1$ distinct nucleotides and a relation between them [e.g., the consensus sequence in the mRNA translation (i), the poly(A) tail in item (ii), and the miRNA seed in item (iii)], (b) aperiodicity theory, which connects “healthy groups” f_p to free groups F_r of rank r and their profinite completion \hat{F}_r , and (c) the representation theory of groups f_p over the space-time-spin group $SL_2(\mathbb{C})$, highlighting the role of surfaces with isolated singularities in the character variety. Our approach could potentially contribute to the understanding of the molecular mechanisms underlying various diseases and help develop new diagnostic or therapeutic strategies.

1

Keywords: RNA metabolism; micro-RNAs; diseases; finitely generated group; $SL_2(\mathbb{C})$ character variety; aperiodicity.

1. INTRODUCTION

Genome-scale metabolic pathways [1, 2], genome–environment interactions [3], the immune response [4], post-transcriptional regulatory mechanisms [5] and oncohistones [6] represent aspects of a research field connecting the heritable genetic code to other biological codes.

The aforementioned genetic code is defined precisely as a non-injective map from the 64 codons to the 20 amino acids. Both finite groups [7, 8, 9] and quantum groups [10] play a leading role in modeling this code. More explicitly, in our paper [8], complete quantum information is encoded in

[†] Université de Franche-Comté, Institut FEMTO-ST CNRS UMR 6174, 15 B Avenue des Montboucons, F-25044 Besançon, France. michel.planat@femto-st.fr.

[‡] Quantum Gravity Research, Los Angeles, CA 90290, USA.
davidc@QuantumGravityResearch.org; Marcelo@quantumgravityresearch.org;
raymond@QuantumGravityResearch.org; Fang@QuantumGravityResearch.org;
Klee@quantumgravityresearch.org.

the 22 irreducible characters of the small group $(240, 105) \cong \mathbb{Z}_5 \rtimes 2O$, with $2O$ the binary octahedral group. The characters are put in correspondence with the DNA multiplets encoding the proteinogenic amino acids and the multiplicity is reflected in the dimension of the character representation. Further developments are explored in [11] showing that the small group $(336, 118) \cong \mathbb{Z}_7 \rtimes 2O$ is another model of the genetic code reflecting the symmetry of Lsm1 – 7 complex in the spliceosome. The 8-fold symmetric histone complex is investigated in [12] with the character table of the group $(384, 5589) \cong \mathbb{Z}_8 \rtimes 2O$. The latest papers inaugurate the role played by a specific algebraic surface called the Kummer surface in the quantum modeling of the genetic code.

From now, we refer to the “epigenetic code” as all processes that reveal and execute gene expression. This includes DNA methylation processes [13], mRNA translation preparation, the poly(A) tail, the RNA-induced silencing complex (RISC) — a vital tool in gene regulation comprising single strands of RNA (ssRNA) and double strands of small interfering RNA (siRNA) — and other regulatory nucleotide sequence fragments that are discarded after splicing. For a relation between the epigenetic code and morphogenesis, see [14].

Chemical modifications in RNA also drive the metabolism of transcription of the genetic information. Post-transcriptional regulation in gene expression is a hot topic known as epitranscriptomics. There are more than 170 known types of RNA methylation processes but the most common in eukaryotes is the possible methylation of $\underline{A} = m^6A$ on sites with a specific short sequence $RR\underline{A}CH$ ($R = A$ or G , $H = A, U$ or C), see e.g. [15, 16, 17].

For studying the epigenetic code (hereinafter referred to as the e-code), we employ infinite (finitely generated) groups denoted by f_p , and their representations over the (2×2) matrix group $SL_2(\mathbb{C})$, where the entries are complex numbers [19]. The significance of this group extends across all fields of physics as it represents a space-time-spin group. In this study, we apply a mathematical field known as algebraic geometry to define the e-code. This has never been done before.

Our crucial observation is that an f_p group associated with a “healthy” sequence usually approximates a free group F_r , where the rank r equals the number of distinct nucleotides (nt) minus one. A sequence deviating from this may suggest a potential e-code deregulation leading to a disease. However, an f_p group closely resembling a free group does not provide sufficient assurance against a disease. Additional examination of the $SL_2(\mathbb{C})$ representations of f_p — termed the character variety — specifically, its basis — called a Groebner basis \mathcal{G} — is necessary.

The Groebner basis comprises a set of surfaces. A surface within \mathcal{G} containing isolated singularities indicates another potential disease that can be identified specifically, e.g., relating to an oncogene or a neurological disorder [19, Figure 6, Tables 2 to 4]. The e-code we define comprises such algebraic geometric characteristics.

An additional attribute of “healthy” sequences, which leads to a group f_p approximating the free group F_r and not mentioned in [19], is their connection to aperiodicity. Schrödinger’s book [20] proposes aperiodicity of living

“crystals”. Our paper [21] characterizes aperiodic DNA sequences. We further this concept by introducing the so-called profinite completion \hat{F}_r of the free group F_r . A sequence $f_p^{(l)}$ of finitely generated groups approaching F_r emerges by applying l repeated substitutions to the generators of f_p . However, all distinct groups $f_p^{(l)}$ should possess the same profinite completion \hat{F}_r . Profinite groups \hat{F}_1 (corresponding to sequences containing two distinct nt) and \hat{F}_2 (corresponding to sequences containing three distinct nt) have been examined in a prominent algebraic geometry treatise [22]. We present the details below in a manner that is accessible to a non-specialist reader.

In Section 2, we illustrate our mathematical concepts through a few simple pedagogical examples. In Section 3, we apply these concepts to the cases of mRNA translation, microRNAs and m^6A methylation. In Section 4, we provide additional comments, a summary diagram and perspectives.

2. METHODS AND PRELIMINARY RESULTS

2.1. Infinite finitely generated groups f_p and free groups F_r .

The TATA box. We’ll start with a simple example of an infinitely finitely generated group taken from the context of introns. The DNA sequence located in the core promoter region of many eukaryotic genes is the Goldberg-Hogness sequence, also known as the TATA box. This sequence contains a non-coding segment with repeated T and A base pairs. The TATA box serves as the binding site for the TATA-binding protein and other transcription factors in some eukaryotic genes. Its consensus sequence takes the form rel=TATAAAA. Variations in this consensus sequence, resulting from genetic polymorphism, can lead to diseases like Gilbert’s syndrome and immune suppression [23].

In our methodology, we define the group $f_p = \langle A, T | \text{rel} \rangle$, which contains infinitely many elements. There are numerous ways to investigate this group, but we opted for a specific one. This method involves calculating the number of conjugacy classes of subgroups of index d of f_p (a sequence we’ll refer to as the card seq of f_p). The card seq of f_p for the selected TATA sequence is $[1, 1, 2, 3, 2, 8, 7, 10, 18, 28 \dots]$. Interestingly, the group $H_3 = \langle A, T | A^2 = T^3 \rangle$ shows a similar card seq (at least up to the highest index we can reach with the calculations). The group H_3 , as defined, is isomorphic to the so-called modular group $PSL(2, \mathbb{Z})$ – the group of (2×2) matrices of determinant 1 with integer entries. This group has an intriguing topological interpretation as the fundamental group of the trefoil knot manifold. Thus, we find that the group f_p is ‘close’ to H_3 since the card seq of both groups is the same, but we can easily verify that f_p and H_3 are not isomorphic.

In paper [25, Section 3.1 and Table 2], we discovered that Hecke groups $H_q = \langle A, T | A^2 = T^q \rangle$, with $q = 3$ or 4 , have a card seq corresponding to ‘healthy’ TATA box sequences. The f_p group for a TATA box with a card seq resembling that of Hecke groups, with $q \neq 3$ or $q \neq 4$, or even that of groups slightly different from H_3 and H_4 , signifies Gilbert’s syndrome.

Polyadenylation signals. For our second example, we select a sequence from the context of eukaryotic polyadenylation [24]. Polyadenylation involves the addition of a poly(A) tail to an RNA transcript, usually a messenger RNA (mRNA). A consensus poly(A) sequence takes the form $\text{rel1}=\text{AAUAAA}$. This corresponds to a two-generator group of the form $f_p = \langle AU|\text{rel1} \rangle$. The card seq of such a group is found to be $[1, 1, 1, 1, 1, 1, 1, 1, 1, 1, \dots]$, implying a single conjugacy class for each index. It appears that the free group $F_1 = \langle A, U|AU \rangle$, of rank 1, has the same card seq as the f_p group with relation rel1 , even though both groups are not isomorphic.

Another consensus poly(A) sequence takes the form $\text{rel2}=\text{UGUAA}$. This corresponds to a three-generator group of the form $f_p = \langle A, U, G|\text{rel2} \rangle$. The card seq of such a group is found to be $[1, 3, 7, 26, 97, 624, 4163, \dots]$. Intriguingly, the free group $F_2 = \langle A, U, G|AUG \rangle$, of rank 2, has the same card seq as the f_p group with relation rel2 , despite both groups not being isomorphic.

From our perspective, DNA/RNA sequences that lead to f_p groups closely resembling a free group are considered 'healthy' sequences [19, 21, 25]. The standard poly(A) sequences mentioned earlier play a regulatory role in producing mature mRNA during translation. Sequences that generate an f_p group diverging from a free group F_r may be indicative of a disease.

2.2. Aperiodic sequences, their attached groups f_p and free groups.

In this subsection, we'll elucidate how a group f_p , with a card seq identified to be close to a free group F_r , can be linked to an aperiodic sequence and the profinite completion \hat{F}_r . We introduced the concept of aperiodic groups and sequences in our earlier papers [25, Section 4] and [21, Section 2].

Consider the motif $\text{rel} = \text{TTTATTA}$, which serves as a consensus sequence for the transcription factor of the DBX gene in *Drosophila melanogaster* (fruit flies). This gene is involved in neuronal specification and differentiation. The group $f_p = \langle A, T|\text{rel} \rangle$ has the same card seq as the free group F_1 of rank 1. Furthermore, by splitting rel into two segments $\text{rel} = \text{rel}_A \text{rel}_T$ and applying the substitution maps $A \rightarrow \text{rel}_A = \text{TTTA}$, $T \rightarrow \text{rel}_T = \text{TTA}$, we generate the substitution sequence

$$S_{DBX} = A, T, AT, TTTATTA, TTATTATTATTTATTATTATTTA, \dots$$

Upon inspection, it's straightforward to observe that all finitely generated groups $f_p^{(l)}$, with their generators being

$AT, TTTATTA, TTATTATTATTTATTATTATTTA, \dots$, respectively, possess the card seq of F_1 .

As per Reference [25, Section 4], a substitution rule to be considered aperiodic must satisfy two conditions: (1) the substitution matrix M must be primitive, meaning it should be a strictly positive matrix (all entries > 0), irreducible, and M^k should be strictly positive for some k . This condition is denoted as $M \gg 0$, and (2) the Perron-Frobenius λ_{PF} eigenvalue must be irrational. It's worth noting that the Perron-Frobenius eigenvector of an irreducible non-negative matrix is the only one whose entries are all positive.

The aforementioned sequence has a substitution matrix $M = \begin{pmatrix} 1 & 3 \\ 1 & 2 \end{pmatrix}$.

One can verify that M is primitive since $M^2 \gg 0$ and $\lambda_{PF} = (3 + \sqrt{13})/2$. Conditions (1) and (2) are satisfied, implying that the substitution S_{DBX} is aperiodic.

Numerous other genes have transcription factors with a motif rel generating an aperiodic sequence [21, Table 2].

2.3. Aperiodic sequences and the profinite groups \hat{F}_r . This section can be skipped without affecting the comprehension of the rest of the paper. It endeavors to answer the following question: why do the aforementioned groups $f_p^{(l)}$ produce the same card seq as that of the free group F_1 ? The tentative answer to this question is that the profinite completion of all groups $f_p^{(l)}$ is the profinite group \hat{F}_1 . By making this observation, we align the aperiodicity of sequences with profinite groups. Profinite groups were introduced by Grothendieck in the context of algebraic geometry [22]. Here, we describe the necessary ingredients for the layperson, focusing first on \hat{F}_1 and then on \hat{F}_2 , and their relevance to our present work.

A group G can be considered a 'topological group' by applying the 'discrete topology', in which the elements of G are points of a 'discrete space', form a 'discontinuous sequence' and are isolated from each other. Every subset is 'open' in the discrete topology. A profinite group is a topological group that, in a certain sense, is assembled from a system of finite groups. A profinite group requires a system of finite groups and group homomorphisms between them.

Given a group G , there is a related profinite group \hat{G} defined as the inverse limit $\hat{G} = \lim_{\leftarrow} G/N$, of the groups G/N , where N runs through the normal subgroups of G of finite index [a normal subgroup is a subgroup that remains invariant under conjugation by members of the group]. Each finite quotient group corresponds to a normal subgroup N of G and the profinite completion \hat{G} can be perceived as containing an analogue of each of these normal subgroups.

The profinite group \hat{G} exhibits several properties: it is non-abelian, residually finite [meaning that for any non-identity element g in \hat{G} , there exists a finite quotient of \hat{G} in which g is not the identity], and totally disconnected [meaning that the only connected subsets of \hat{G} are singletons, sets containing only one element].

In general, an explicit construction of profinite groups \hat{G} cannot be obtained. However, \hat{F}_1 and \hat{F}_2 are not overly complex to handle.

About the profinite group \hat{F}_1 . Let's begin with \hat{F}_1 . The free group F_1 on a single generator can be described as a group with one generator, say a , and no relations. It consists of all possible finite strings that can be formed by combining the generator and its inverse. It is the infinite cyclic group $Z = \{1, a, a^{-1}, a^2, a^{-2}, a^3, a^{-3}, \dots\}$. Now, let's discuss the profinite completion of F_1 . The profinite group \hat{F}_1 is isomorphic to the group of all units of the commutative ring of p-adic integers Z_p , across all primes p . It is often denoted as Z_p^* since it corresponds to the elements of Z_p with a valuation of zero. The p-adic integers are a special class of numbers utilized in number theory and algebraic geometry.

About the profinite group \hat{F}_2 . Let's briefly discuss \hat{F}_2 . This topic was initiated in [22]. The subject is complex. It's connected to the so-called Belyi

theorem, a fundamental result that establishes a connection between algebraic curves defined over the algebraic closure of the rationals, $\bar{\mathbb{Q}}$, and certain rational functions called Belyi functions.

An algebraic curve defined over $\bar{\mathbb{Q}}$ can be represented as a branched covering of the Riemann sphere (the complex projective line $\mathbb{P}^1(\mathbb{C})$) branched only over three points (usually taken as 0, 1, and ∞) if and only if the curve itself is defined over a number field, which is a finite extension of the field of rational numbers \mathbb{Q} .

In other words, the Belyi theorem implies that an algebraic curve defined over a number field can be mapped to the Riemann sphere in such a way that the ramification (branching) is restricted to just three points. The rational functions that provide these branched coverings are known as Belyi functions.

The significance of the Belyi theorem lies in the fact that it provides a method to study algebraic curves defined over number fields by analyzing their ramified coverings and the associated dessins d'enfants, which are combinatorial objects encoding the ramification data.

Specifically, we have the crucial result that

$$\hat{\pi}_1(\mathbb{P}^1(\mathbb{C}) \setminus \{0, 1, \infty\}) \cong \hat{F}_2,$$

i.e., the so-called étale fundamental group for the triply branched projective line is the profinite group \hat{F}_2 .

2.4. $SL_2(\mathbb{C})$ representations of groups f_p and a Groebner basis \mathcal{G} .

While the previous section about profinite groups showcases the importance of algebraic geometry in the context of DNA/RNA sequences, it remains somewhat abstract. To address this, we can consider the representations of an f_p group over the space-time-spin group $SL_2(\mathbb{C})$, as we did in [18, 19, 21].

Representations of f_p in $SL_2(\mathbb{C})$ are homomorphisms $\rho : f_p \rightarrow SL_2(\mathbb{C})$ with character $\kappa_\rho(g) = \text{tr}(\rho(g))$, $g \in f_p$. The notation $\text{tr}(\rho(g))$ signifies the trace of the matrix $\rho(g)$. The set of characters is employed to determine an algebraic set by taking the quotient of the set of representations ρ by the group $SL_2(\mathbb{C})$, which acts by conjugation on representations [26, 27].

In such papers, we elaborated that the character variety of f_p is a set comprised of a sequence X of multivariate polynomials. A particular basis related to X is the Groebner basis $\mathcal{G}(X)$, whose factors define hypersurfaces.

Our precursor paper [18] focused on a possible algebraic approach of topological quantum computing. Later, in [19, 21], we could investigate $SL_2(\mathbb{C})$ representations of short DNA/RNA sequences (e.g. the consensus sequence of a transcription factor or the seed of a microRNA) and relate them to a potential disease.

For a two-generator group f_p , the factors are three-dimensional surfaces. In general, these surfaces can be classified by mapping them to a rational surface across five categories [19, Section 3]. Often encountered surfaces are degree p Del Pezzo surfaces where $1 \leq p \leq 9$. A rational surface may either be non-singular, 'almost non-singular', having only isolated singularities, or singular. Almost non-singular surfaces are crucial in our context. A simple singularity is referred to as an A-D-E singularity and must be of the type A_n , $n \geq 1$, D_n , $n \geq 4$, E_6 , E_7 or E_8 .

The A-D-E type is mirrored in the notation we employ. For instance, $S^{(lA_1, mA_2, nA_3, \dots)}$ denotes a surface containing l type A_1 , m type A_2 , n type A_3 singularities, etc. A generic surface is the Cayley cubic we encountered in our previous papers, defined as $S^{(4A_1)} = xyz + x^2 + y^2 + z^2 - 4$ [19, Figure 5].

For a three-generator group f_p , the factors of $\mathcal{G}(X)$ are seven-dimensional surfaces of the form $S_{a,b,c,d}(x, y, z)$. Some of them belong to the Fricke family [19, Equation 3], which is associated with the four-punctured sphere. But for a chosen set of parameters a, b, c, d , the hypersurface reduces to an ordinary three-dimensional surface.

For a four-generator group f_p , the factors of $\mathcal{G}(X)$ are 14-dimensional surfaces containing 4 copies of the form $S(x, y, z)$, $S(x, u, v)$, $S(y, u, v)$ and $S(z, v, w)$ for selected choices of 8 parameters.

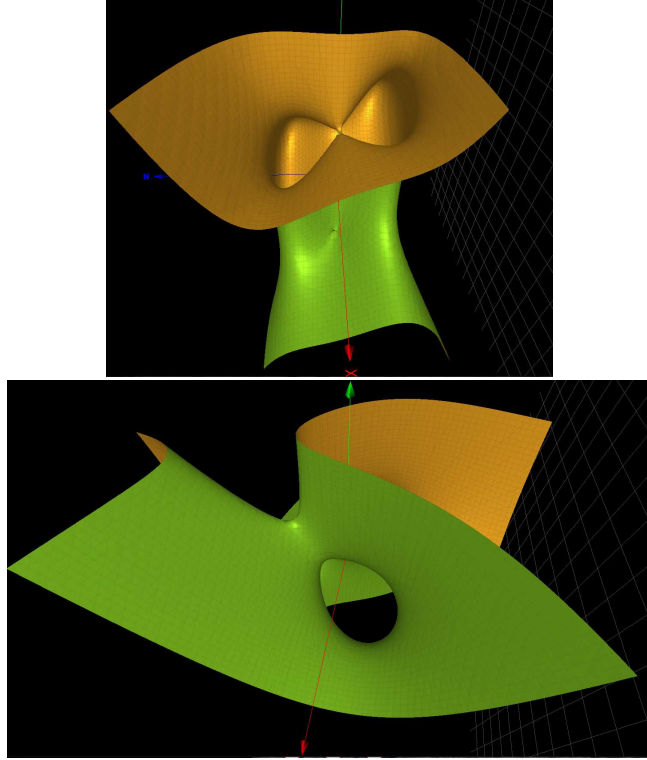


FIGURE 1. Up: The degree 2 Del Pezzo surface within \mathcal{G}_{TATA} . Down: The degree 3 Del Pezzo surface $S^{(A_1)}$ within $\mathcal{G}_{\text{rel1}}$.

Groebner basis for the TATA box. The Groebner basis for the character variety associated with the f_p group of generator $\text{rel}=\text{TATAAAA}$ of the TATA box, studied in subsection 2.1, is found to be:

$$\mathcal{G}_{TATA} = (z^4 - xy^2 - xyz + x^2 + y^2 + yz - 3z^2 + x - 2)(x^2z - xy - xz + y - z) \\ S^{(A_2)}S^{(A_4)}(x^3 - z^2 - 3x + 2),$$

where $S^{(A_2)} = x^2y - z^3 - xz - y + 3z$ and $S^{(A_4)} = xz^2 - x^2 - yz - x + 2$ are degree 3 Del Pezzo surfaces.

The Groebner basis \mathcal{G}_{TATA} comprises a degree 2 Del Pezzo surface (see Fig. 1, up), and a rational scroll whose analytic expression is in the first row. Both surfaces are singular. The second row consists of two surfaces with simple singularities of type A_2 and A_4 , respectively. The last term represents a curve (not a surface).

Groebner basis for polyadenylation signals. For the first polyadenylation signal considered in subsection 2.1, the relation of the f_p group is $\text{rel1}=\text{AAUAAA}$. The corresponding Groebner basis is:

$$\mathcal{G}_{\text{rel1}} = 3 \text{ rational scrolls} \times P^2 \times S^{(4A_1)}S^{(A_1)} \times \text{curve}.$$

The Groebner basis $\mathcal{G}_{\text{rel1}}$ contains three rational scrolls, a surface birationally equivalent to the projective plane P^2 , the Cayley cubic $S^{(4A_1)}$, the degree 3 Del Pezzo surface $S^{(A_1)} = x^2y - xz^2 - xz + yz + x - y$ (see Fig. 1, down) and a curve.

For the second polyadenylation signal considered in subsection 2.1, the relation of the f_p group is $\text{rel2}=\text{UGUAA}$. The factors of $\mathcal{G}(X)$ are seven-dimensional hypersurfaces $S_{a,b,c,d}(x, y, z)$. However, choosing specific parameters, such as $S_{0,0,0,0}(x, y, z)$ or $S_{1,1,1,1}(x, y, z)$, we obtain three-dimensional surfaces. These are found to be degree 3 Del Pezzo surfaces with simple singularities of the form S^{lA_2} , with $l=1, 2$ or 3 , quadrics, or curves.

Groebner basis for the transcription factor of DBX gene. For the DBX gene studied in Section 2.2, the Groebner basis takes the form

$\mathcal{G}_{DBX} = \text{scroll} \times P^2 \times S^{(A_4)} \times S^{(A_2)} \times S^{(4A_1)} \times \text{curve}$, where $\text{scroll} = y^2z - xy - yz + x - z$ and $P^2 = z^4 - x^2y + xz - 4z^2 + y + 2$ are singular. The other factors are DP^3 surfaces with isolated singularities that are $S^{(A_4)} = yz^2 - y^2 - xz - y^2$, $S^{(A_2)} = z^3 - xy^2 + yz + x - 3z$, the Cayley cubic $S^{(4A_1)}$ and curve $= y^3 - z^2 - 3y + 2$.

3. FURTHER RESULTS

In this section, we produce further results related to mRNA metabolism and miRNA.

3.1. Algebraic geometry of mRNA translation.

The Shine-Dalgarno box. Ribosomal RNA (rRNA) – a type of non coding RNA – is the main component of a macromolecular machine, called the ribosome, whose role is to ensure mRNA translation. The initiation of translation needs the recognition of the appropriate sequences on the m-RNA by the ribosome. A major factor in this recognition is an mRNA-rRNA interaction first proposed by Shine and Dalgarno [28]. They proposed that the ribosomal nucleotides recognize the complementary purine-rich sequence $\text{rel3}=\text{AGGAGGU}$, which is found around 8 bases upstream of the start codon AUG in a number of mRNAs found in viruses that affect Escherichia coli.

Let us study the group $f_p = \langle A, G, U | \text{rel3} \rangle$. The card seq of f_p is found to be the same than that of the free group F_2 .

The $SL_2(\mathbb{C})$ character variety is a scheme X whose a Groebner basis $\mathcal{G}(X)$ is made of of 7-dimensional surfaces $S_{a,b,c,d}(x, y, z)$. By projecting to 3 dimensions, one gets surfaces like $S_{0,0,0,0}(x, y, z)$ and $S_{1,1,1,1}(x, y, z)$ as in Section 2.4. We find degree 3 Del Pezzo surfaces with isolated singularities $S^{(A_1)} = x^2y + yz^2 + 4xz + 4y$ and $x^2y + yz^2 + x^2 + z^2 + 6xz + 5y - 6z - 7$, $S^{(A_2)} = xyz + 2x^2 + z^2 + 4$ and $S^{(A_4)} = xyz + 3x^2 + z^2 - 5z$, quadrics and curves.

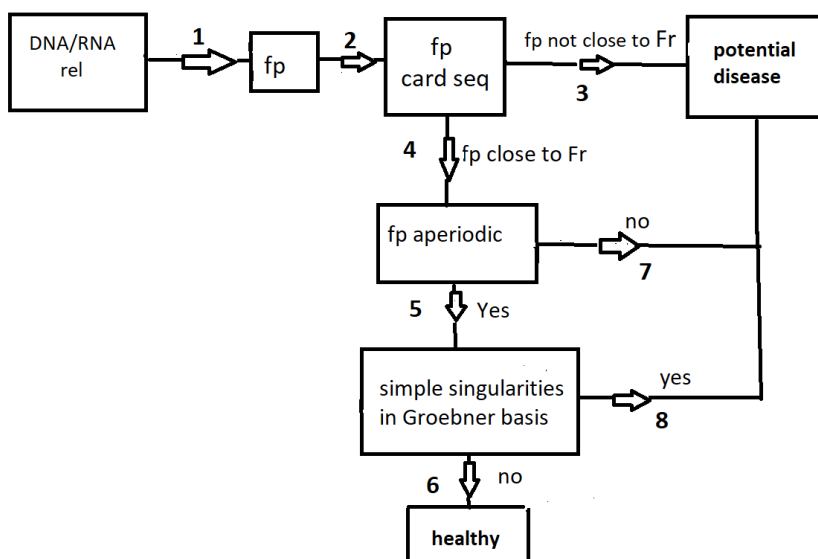


FIGURE 2. A diagram illustrating the main results discussed in the text. For example, for the transcription factor of the gene EGR1, $rel=GCGTGGGCG$ [25, Section 4.1.2], the path is $1 \rightarrow 2 \rightarrow 4 \rightarrow 5 \rightarrow 6$ showing no risk of disease. But for the transcription factor of gene DBX (see Section 2.2 and 2.4), $rel=TTTATTA$, the path is $1 \rightarrow 2 \rightarrow 4 \rightarrow 5 \rightarrow 8$ meaning a potential disease (see Table 1).

Kozak consensus sequence. The Kozak consensus sequence is a nucleotide motif that functions as the protein translation initiation site in most eukaryotic mRNA transcripts [29]. The small (40S) subunit of eukaryotic ribosomes bind, initially at the capped 5'-end of messenger RNA and then migrate, stopping at the first AUG codon in a favorable context for initiating translation. In eukaryotes, the Kozak sequence ensures that a protein is correctly translated from the genetic message, mediating ribosome assembly and translation initiation. A sequence logo of the most conserved bases around the initiation codon AUG for human mRNAs may be found in the first caption of [30] as $rel4 = ACCAUGGC$.

Let us study the group $f_p = \langle A, C, G, U | rel4 \rangle$. The card seq of f_p is found to be the same than that of the free group F_3 of rank 3. This group can be linked to an aperiodic sequence by following the steps given in Section 2.2.

By splitting rel4 into four segments $\text{rel4} = \text{rel}_A \text{rel}_C \text{rel}_G \text{rel}_U$ and applying the substitution maps $C \rightarrow \text{rel}_C = A$, $A \rightarrow \text{rel}_A = \text{CCAUG}$, $U \rightarrow \text{rel}_U = G$, $G \rightarrow \text{rel}_G = C$, we generate the substitution sequence

$$S_{\text{Kozak}} = C, A, U, G, \text{CAUG}, \text{ACCAUGGC}, \text{CCAUGA}^2 \text{CCAUGGC}^2 A, \dots$$

Upon inspection, it's straightforward to observe that all finitely generated groups $f_p^{(l)}$, with their generators being

$\text{CAUG}, \text{ACCAUGGC}, \text{CCAUGA}^2 \text{CCAUGGC}^2 A, \dots$, respectively, possess the card seq of F_3 .

The aforementioned sequence has a substitution matrix $M = \begin{pmatrix} 0 & 2 & 0 & 1 \\ 1 & 1 & 0 & 0 \\ 0 & 1 & 0 & 0 \\ 0 & 1 & 1 & 0 \end{pmatrix}$.

One can verify that M is primitive since $M^4 \gg 0$ and $\lambda_{PF} \approx 2.2055694$ is the only real (and irrational) solution of the equation $x^3 - 2x^2 - 1$. Conditions (1) and (2) of Section 2.2 are satisfied, implying that the substitution S_{Kozak} is aperiodic. See [31] for a connection of the later Perron-Frobenius eigenvalue to random Fibonacci sequences.

Mutation of a purine at position -3 with respect to the AUG codon is known to be associated to a disease such as a type of thalassemia due to a bad initiation of α -globin [29]. In our approach the mutation from rel4 to $\text{rel4}' = \text{CCCAUGGC}$ leads to a substitution M' that is no longer primitive so that the property of aperiodicity of the sequence is lost. However the cardseq of the associated f_p group is still that of the free group F_3 . No other substitution in the sequence $\text{rel4}'$ can be found to restore the aperiodicity.

3.2. Algebraic geometry of miRNAs. A microRNA (miRNA) is a small, single-stranded, non-coding RNA molecule containing approximately 22 nucleotides. miRNAs play crucial roles in RNA silencing and post-transcriptional regulation of gene expression by specifically targeting certain mRNAs for degradation and translational repression [32, 33]. miRNA genes are typically transcribed by RNA polymerase II (Pol II), which binds to a promoter located near the DNA sequence, encoding what will become the hairpin loop of a pre-miRNA (for precursor-miRNA). The pre-miRNAs are approximately 70 nucleotides in length and fold into imperfect stem-loop structures.

A miRNA consists of a duplex comprising two strands ($-5p$ and $-3p$). However, a single strand is selected into the RNA-induced silencing complex to serve as a template during the transcript of a complementary mRNA [34, 35]. For details about the miRNA sequences, we use the Mir database [36, 37, 38].

It should be emphasized that a given miRNA may have hundreds of different mRNA targets, and a single target might be regulated by multiple miRNAs.

For previous results about how to define a f_p group from the seed of a miRNA, the reader may consult [19, Section 4.3].

Below, we focus on other examples.

miRNA hsa-mir-122. Mir-122 is a tissue specific miRNA which is highly expressed in liver [39, Figure 5]. It is involved in cholesterol accumulation

and fatty acid metabolism. It has a leading role in controlling hepatitis C virus (HCV) [40, 41].

The seed region for mir-122-5p is seed0=GGAGUGU. The corresponding group $f_p = \langle C, G, U | \text{seed0} \rangle$ has the card seq of the free group F_2 .

Let us first check if the seed sequence is aperiodic. By splitting seed0 into three segments seed0= seed_Aseed_Gseed_U and applying the substitution maps $A \rightarrow \text{seed}_A = GG$, $G \rightarrow \text{seed}_G = AGU$, $U \rightarrow \text{seed}_U = GU$, one can check that the finitely generated groups $f_p^{(l)}$ with generators

$$GGAGUGU, AGUAGUGGAGUGUAGUGU, \dots$$

possess the card seq of the free group F_2 . Following the method described

in Section 2.2, one gets the (primitive) substitution matrix $M = \begin{pmatrix} 0 & 1 & 0 \\ 2 & 1 & 1 \\ 0 & 1 & 1 \end{pmatrix}$

whose characteristic polynomial $\lambda^3 - 2\lambda^2 - 2\lambda + 2$ has three real roots. The largest one is the (irrational) Perron-Frobenius eigenvalue $\lambda_{PF} \approx 2.481194$. One concludes the sequence seed0 is aperiodic.

Let us now look at the Groebner basis for the $SL_2(\mathbb{C})$ representation of f_p with the method described in Section 2.4. One obtains $\mathcal{G}_{\text{mir-122-5p}}(0, 0, 0, 0) = 8yz(2 - z^2)$ and $\mathcal{G}_{\text{mir-122-5p}}(1, 1, 1, 1) = -4z^2(x - z^2 + z + 1)(y + z^3 - z^2 - 2z)$. One can check that for all values of the parameters $\mathcal{G}_{a,b,c,d}(x, y, z)$ only contains factors which are curves (not surfaces).

miRNA hsa-mir-503. The slowest evolving miRNA gene in the human species (hsa) is hsa-mir-503 [37]. It regulates gene expression in various pathological processes of diseases, including carcinogenesis, angiogenesis, tissue fibrosis, and oxidative stress [42].

The seed region for mir-503-5p is seed1=AGCAGCGG. The corresponding group $f_p = \langle A, C, G | \text{seed1} \rangle$ has the card seq of the free group F_2 . For this group, the Groebner basis with parameters $(a, b, c, d) = (0, 0, 0, 0)$ is quite simple: $\mathcal{G}_{\text{mir-503-5p}}(0, 0, 0, 0) = S^{(4A_1)}(x, y, z)$, which is the already mentioned Cayley cubic.

For $(a, b, c, d) = (1, 1, 0, 0)$, $\mathcal{G}_{\text{mir-503-5p}}(1, 1, 0, 0) = -3xyz\kappa_3(x, y, z)$, where $\kappa_3(x, y, z)$ is the Fricke surface found in [43, Section 3.3]. For $(a, b, c, d) = (1, 1, 1, 1)$, there are several more polynomials. One of them defines the Fricke surface $xyz + x^2 + y^2 + z^2 - 2x - y - 2$.

The considered seed region for mir-503-3p is GGGUAUU. The surfaces in the Groebner basis are very simple in this case, and no simple singularities exist within them.

miRNA hsa-mir-146a. Mir-146 is primarily involved in the regulation of inflammation and other processes functioning in the innate immune system. It plays a role in neuropathogenesis.

The considered seed region for hsa-mir-146a-5p is seed2=GAGAAC [37]. Again the corresponding group $f_p = \langle A, C, G | \text{seed2} \rangle$ has the card seq of the free group F_2 .

The Groebner basis with parameters $(a, b, c, d) = (0, 0, 0, 0)$ is

$$\mathcal{G}_{\text{hsa-146a-5p}}(1, 1, 1, 1) = (xz + y + 2)(y - z^2 + 2)^2(x^2 + z^2 - 2y - 4)S^{(3A_2)},$$

where $S^{(3A_2)} = z^3 - xy - 2yz - 2x - 4z$.

The Groebner basis with parameters $(a, b, c, d) = (1, 1, 1, 1)$ is of the form

$\mathcal{G}_{hsa-146a-5p}(1, 1, 1, 1) = DP^4 \times f^{(2A_2)} \times \text{quadric} \times \text{curves}$, where DP^4 is a degree 4 del Pezzo surface.

miRNAs and disease. As we announced earlier (see also [19]), a potential disease is associated with f_p groups which fail to satisfy at least one of three requirements (1) the card seq of f_p should be that of a free group F_r , (2) the generating sequence should be aperiodic, (3) the $SL_2(\mathbb{C})$ character variety of f_p should have a Groebner basis devoid of isolated singularities (even though the f_p group may have the card seq of a free group [19, Figure 6]).

Following this criteria, the sequence hsa-mir-122-5p is healthy while the sequences hsa-mir-503-5p and hsa-mir-146a-5p are not since the criterion (3) is not satisfied. Additional examples can be found in [19, Table 3].

Besides isolated singularities, the Groebner basis may contain singular surfaces that are not simply singular. The DP^4 surface in $\mathcal{G}_{hsa-146a-5p}(1, 1, 1, 1)$ is an example of a singular surface. Further mathematical techniques are required to investigate these surfaces [44]. However, we will not discuss these methods in this paper.

TABLE 1. A few possible paths in the diagram of Figure 2 terminating at 6 (healthy) or (3)-(7)-(8) (potential disease). The set $\{6, 8\}$ denotes a lack of a clear conclusion about the existence of an isolated singularity. The selected examples are taken in three parts that are transcription factors (group 1), regulating elements in introns (group 2) and miRNAs (group 3). Details are given in the text. Otherwise a reference is provided.

Sequence	rel	path
EGR1 [25]	GCGTGGGCG	$1 \rightarrow 2 \rightarrow 4 \rightarrow 5 \rightarrow 6$
FOS [25]	TGAGTCA	$1 \rightarrow 2 \rightarrow 4 \rightarrow 5 \rightarrow \{6, 8\}$
Nanog [25]	TAATGG	$1 \rightarrow 2 \rightarrow 4 \rightarrow \{7, 8\}$
DBX	TTTATTA	$1 \rightarrow 2 \rightarrow 4 \rightarrow 5 \rightarrow 8$
TATA	TATAAAA	$1 \rightarrow 2 \rightarrow 3 \rightarrow (7, 8)$
poly(A) (rel1)	AAUAAA	$1 \rightarrow 2 \rightarrow 4 \rightarrow \{7, 8\}$
poly(A) (rel2)	UGUAA	$1 \rightarrow 2 \rightarrow 4 \rightarrow \{7, 8\}$
Shine-Dalgarno (rel3)	AGGAGGU	$1 \rightarrow 2 \rightarrow 4 \rightarrow 5 \rightarrow 8$
Kozak (rel4)	ACCAUGGC	$1 \rightarrow 2 \rightarrow 4 \rightarrow 5 \rightarrow \{6, 8\}$
Kozak (rel4')	CCCAUGGC	$1 \rightarrow 2 \rightarrow 4 \rightarrow 7$
hsa-mir-122-5p [41] (seed0)	GGAGUGU	$1 \rightarrow 2 \rightarrow 4 \rightarrow 5 \rightarrow 6$
hsa-mir-132-5p [45]	CCGUGGC	$1 \rightarrow 2 \rightarrow 4 \rightarrow 5 \rightarrow 6$
hsa-mir-503-5p (seed1) [42]	AGCAGCGG	$1 \rightarrow 2 \rightarrow 5 \rightarrow 8$
hsa-mir-146a-5p (seed2) [46]	GAGAAC	$1 \rightarrow 2 \rightarrow \{7, 8\}$
hsa-mir-7-5p [47]	GGAAGA	$1 \rightarrow 2 \rightarrow \{3, 7, 8\}$
hsa-mir-7-5p	GGAAGAC	$1 \rightarrow 2 \rightarrow 4 \rightarrow 5 \rightarrow 6$
hsa-mir-7-3p	AACAAAU	$1 \rightarrow 2 \rightarrow 4 \rightarrow 7$
hsa-mir-155-3p [35, 46]	UCCUAC	$1 \rightarrow 2 \rightarrow 4 \rightarrow \{7, 8\}$
hsa-mir-155-3p	UCCUACA	$1 \rightarrow 2 \rightarrow 3$

TABLE 2. A detailed group theoretical analysis of m^6A modifications for bacteria (the sequence GCCAG) and eukaryotes (sequence $RRACH$ ($R = A$ or G , $H = A, U$ or C)). Column 2 is the group closer to the f_p group generated by the sequence in column 1 (F_r is for the free group of rank r , H_3 is for the modular group $PSL(2, \mathbb{Z})$). If the sequence is aperiodic, the Perron-Frobenius eigenvalue λ_{PF} is given in column 3. The type of isolated singularity, if any, is in column 4. The path in the diagram of Figure 2 is shown in column 5.

Sequence	group	aperiodic	Groebner basis	path
bacterial GCCAG	F_2	1.83928	no	$1 \rightarrow 2 \rightarrow 4 \rightarrow 5 \rightarrow 6$
eukaryote AAACA	F_1	no	$S^{(A_2)}, S^{(A_1A_2)}$	$1 \rightarrow 2 \rightarrow 4 \rightarrow \{7, 8\}$
AAACC	H_3	no	no	$1 \rightarrow 2 \rightarrow \{3, 7\}$
AAACU	F_2	no	no	$1 \rightarrow 2 \rightarrow 4 \rightarrow 7$
GGACA	F_2	1.83928	$S^{(A_2)}, S^{(A_2A_2)}$	$1 \rightarrow 2 \rightarrow 4 \rightarrow 5 \rightarrow 8$
GGACC	F_2	no	no	$1 \rightarrow 2 \rightarrow 4 \rightarrow 7$
GGACU	F_3	no	unknown	$1 \rightarrow 2 \rightarrow 4 \rightarrow 7$

4. DISCUSSION

In this section, we summarize our paper by referring to the diagram in Figure 2. Given a short DNA/RNA sequence, rel , which represents a consensus sequence in a transcription factor, the seed of a miRNA, or a relevant sequence in mRNA recognition and processing, we construct a finitely generated group, f_p . The architecture of subgroups, card seq, within this group is computed (see Section 2.1). If the f_p card seq matches that of the free group F_r (of rank r equal to $nt-1$), we proceed to path 4; otherwise, a potential disease could be in sight (path 3). After reaching path 4, the next step involves checking the aperiodicity of rel and the corresponding f_p group, as described in Section 2.2. The final step is to examine the presence (or absence) of isolated singularities in the Groebner basis \mathcal{G} for the $SL_2(\mathbb{C})$ character variety associated with f_p , as outlined in Section 2.4. For a healthy sequence, the path concludes at 6, while a potential disease may be indicated if the path ends at 3, 7 or 8.

In Table 1, we provide several examples of paths. All three checks can be performed, even if paths 4 or 5 are not followed. For instance, the termination $\{7, 8\}$ signifies that the sequence fails both in being aperiodic and in being devoid of simple singularities.

For sequences with 4 distinct nucleotides (like the sequence of transcription factor FOX or the Kozak sequence rel_4), it is difficult to conclude about the risk of a disease. The generic Groebner basis $\mathcal{G}(x,y,z)$ always contains surfaces with isolated singularities such as $S^{(4A_1)}$ and $S^{(3A_1)}$ and there are four copies of them. The termination $\{6, 8\}$ applies for this case.

Algebraic geometry of m^6A modifications. As mentioned in the introduction, a subfield of epigenetics deals about post-transcriptional mRNA modifications. N^6 -methyladenosine (m^6A) is the most frequent modification

in most eukaryotes. But m^6A is also present in bacteria with the consensus motif $GCCAG$ [48, 49]. An interesting aspect is that the mRNA m^6A motif in bacteria is distinct from the consensus motif in eukaryotes ($RRACH$). This features the evolutionary machinery present in the last eukaryotic common ancestor (LECA) compared to the last universal common ancestor (LUCA) [50, Fig. 2].

In Table 2, we provide details about the group generated by these sequences, when the sequence is aperiodic and/or has a Groebner basis of its character variety containing an isolated singularity. As in Table 1, the path in the diagram of Figure 2 is shown.

We clearly read that only the bacterial sequence leads to a path terminating at the edge 6 of the diagram of Figure 2. In the closest eukaryotic sequence GGACA (from the viewpoint of group analysis), isolated singularities are found, such as the degree 3 Del Pezzo surface $S^{(A_2A_2)} = y^3 - 2xz - 4y$. The other sequences are not aperiodic. On the biological point of view, it is known that an appropriate level of m^6A methylation is beneficial but it may be a risk to drive it in an artificial way because it may destroy the delicate balance of regulations performed within the messenger RNA.

Our approach is quite comprehensive and can be applied in numerous contexts beyond those we have considered thus far. It has the potential to impact the search for underlying causes of diseases and aid in the discovery of therapeutic strategies. The e-code, the processes that reveal and execute gene expression, has a sophisticated structure, which our mathematical approach aims to elucidate.

AUTHOR CONTRIBUTIONS

Conceptualization, M.P., F.F. and K.I.; methodology, M.P., D.C. and R.A.; software, M.P.; validation, R.A., F.F., D.C. and M. M.A.; formal analysis, M.P. and M. M.A.; investigation, M.P., D.C., F.F. and M. M.A.; writing—original draft preparation, M.P.; writing—review and editing, M.P.; visualization, F.F. and R.A.; supervision, M.P. and K.I.; project administration, K.I.; funding acquisition, K.I. All authors have read and agreed to the published version of the manuscript.

FUNDING

Funding was obtained from Quantum Gravity Research in Los Angeles, CA.

DATA AVAILABILITY

Computational data are available from the authors.

ACKNOWLEDGMENTS

The first author would like to acknowledge the contribution of the COST Action CA21169, supported by COST (European Cooperation in Science and Technology).

CONFLICTS OF INTEREST

The authors declare no conflict of interest.

REFERENCES

- [1] Gu, C.; Kim G. B.; Kim, W. J.; Kim, H. U.; Lee, S. Y. Current status and applications of genome-scale metabolic models. *Genome Biology* **2019**, *20*, 121.
- [2] Romão, L. mRNA metabolism in health and disease. *Biomedicines* **2022**, *10*, 2262.
- [3] Peedicayil, J. Genome–environment interactions and psychiatric disorders. *Biomedicines* **2023**, *11*, 1209.
- [4] Scharf, S.; Ackerman, J.; Bender, L.; Wurzel, P.; Schäfer, H.; Hansmann, M. L.; Koch, I. Holistic view on the structure of immune response: Petri net model. *Biomedicines* **2023**, *11*, 452.
- [5] Marques, A. R.; Santos, J. X.; Martiniano, H.; Vilela, J.; Rasga, C.; Romão, L.; Vicente, A. M. Gene variants involved in nonsense-mediated mRNA decay suggest a role in autism spectrum disorder. *Biomedicines* **2022**, *10*, 665.
- [6] Wan, Y. C.E. Histone H2B Mutations in Cancer. *Biomedicines* **2021**, *9*, 694.
- [7] Fimmel, E.; Giannerini, S.; Gonzalez, D. L.; Strüngmann. Circular codes, symmetries and transformations. *J. Math. Biol.* **2014**, *70*, 1623–16434.
- [8] Planat, M.; Aschheim, R.; Amaral, M. M.; Fang, F.; Irwin, K. Complete quantum information in the DNA genetic code. *Symmetry* **2020**, *12*, 1993.
- [9] Sanchez, R.; Barreto, J. Genomic abelian finite groups. Available online: <https://doi.org/10.1101/2021.06.01.446543> (accessed on 1 March 2023).
- [10] Frappat, L.; Sciarrino, A.; Sorba, P. Crystalizing the Genetic Code. *J. Biol. Phys.* **2001**, *27*, 1–34.
- [11] Planat, M.; Chester, D.; Aschheim, R.; Amaral, M. M.; Fang, F.; Irwin, K. Finite groups for the Kummer surface: the genetic code and quantum gravity. *Quantum Rep* **2021**, *3*, 68–79.
- [12] Planat, M.; Aschheim, R.; Amaral, M. M.; Fang, F.; Irwin, K. Quantum information in the protein codes, 3-manifolds and the Kummer surface. *Symmetry* **2021**, *13*, 1146.
- [13] Sanchez, R.; Mackenzie, S. A. On the thermodynamics of DNA methylation process. *Scient. Rep.* **2023**, *13*, 8914.
- [14] Bessonov, N.; Butuzova, O.; Minarsky, A.; Penner R.; Soulé, C.; Tosenberger, A.; Morozova, D. Morphogenesis software based on epigenetic code concept. *Comp. Struct. Biotech. J.* **2019**, *17*, 1203–1216.
- [15] Vissers, C.; Sinha, A.; Ming, G. l.; Song H. The epitranscriptome in stem cell biology and neural development. *Neurobiol. Dis* **2020**, *146*, 105139.
- [16] Wang, S.; Lv, Wei, Lv.; Li, T.; Zhang, S.; Wang, H.; Li, X.; Wang, L.; Ma, D.; Zang, Y.; Shen, J. Xu, Y.; Weii W. Dynamic regulation and functions of mRNA m6A modification. *Cancer Cell Int.* **2022**, *22*, 48.
- [17] Widagdo, J.; Wong, J. J.L.; Anggono, V. The m⁶A-epitranscriptome in brain plasticity, learning and memory. *Seminars In Cell and Devt Biol.* **2022**, *125* 110–121.
- [18] Planat, M.; Amaral, M. M; Fang, F.; Chester, D.; Aschheim, R.; Irwin, K. Character varieties and algebraic surfaces for the topology of quantum computing. *Symmetry* **2022**, *14*, 915.
- [19] Planat, M.; Amaral, M. M; Irwin, K. Algebraic morphology of DNA–RNA transcription and regulation. *Symmetry* **2023**, *15*, 770.
- [20] Schrödinger, E. *What Is Life? The Physical Aspect of the Living Cell*; Cambridge University Press: **1944**, Cambridge, UK.
- [21] Planat, M.; Amaral, M. M; Fang, F.; Chester, D.; Aschheim R.; Irwin, K. DNA sequence and structure under the prism of group theory and algebraic surfaces. *Int. J. Mol. Sci.* **2022**, *3*, 13290.
- [22] Grothendieck, A. *Esquisse d'un programme* **1984**, in Geometric Galois Actions I: Around Grothendieck's Esquisse D'un Programme, London Mathematical Society Lecture Note Series, vol. 242, Cambridge University Press Schneps and Lochak **1997**, pp. 243-283. Avalaible online: <http://matematicas.unex.es/~navarro/res/esquisseeng.pdf>.
- [23] TATA Box: Available online: https://en.wikipedia.org/wiki/TATA_box (accessed on 1 September 2021).

- [24] Polyadenylation: Available online: <https://en.wikipedia.org/wiki/Polyadenylation> (accessed on 1 May 2023).
- [25] Planat, M.; Amaral, M. M.; Fang, F.; Chester, D.; Aschheim R.; Irwin, K. Group theory of syntactical freedom in DNA transcription and genome decoding. *Curr. Issues Mol. Biol.* **2022**, *44*, 1417–1433.
- [26] Goldman, W.M. Trace coordinates on Fricke spaces of some simple hyperbolic surfaces. *Eur. Math. Soc.* **2009**, *13*, 611–684.
- [27] Ashley, C.; Burelle J.P.; Lawton, S. Rank 1 character varieties of finitely presented groups. *Geom. Dedicata* **2018**, *192*, 1–19.
- [28] Jacob, W. F. Jacob, Santer, M., Dahlberg, A. E. A single-base change in the Shine-Dalgarno region of 16 rRNA of Escherichia coli affects translation of many proteins. *Proc. Natl. Acad. Sci. USA* **1987**, *84* 4257–4761.
- [29] Kozak, M. The scanning model for translation: an update. *J. Cell Biology* **1989**, *108* 229–241.
- [30] Kozak consensus sequence: Available online: https://en.wikipedia.org/wiki/Kozak_consensus_sequence (accessed on 1 January 2023).
- [31] Rittaud, B. On the average growth of random Fibonacci sequences. *J. Int. Seq.* **2007**, *10* Article 07.2.4.
- [32] microRNA. Available online: <https://en.wikipedia.org/wiki/MicroRNA> (accessed on 1 September 2022).
- [33] Fang, Y.; Pan, X.; Shen, H. B. Recent deep learning methodology development for RNA–RNA interaction prediction. *Symmetry* **2022**, *14*, 1302.
- [34] Medley, C. M.; Panzade G.; Zinovyeva, A. Y. MicroRNA strand selection,: unwinding the rules. *WIREs RNA* **2021**, *12*, e1627.
- [35] Dawson, O.; Piccinini, A. M. miR-155-3p: processing by-product or rising star in immunity and cancer? *Open Biol.* **2022**, *12*, 220070.
- [36] Kozomara, A.; Birgaonu, M.; Griffiths-Jones, S. miRBase: from microRNA sequences to function. *Nucl. Acids Res.* **2019**, *47*, D155–D162.
- [37] miRBase: the microRNA database. Available online: <https://www.mirbase.org/> (accessed on 1 November 2022).
- [38] Fromm, B.; Billipp, T.; Peck, L. E.; Johansen, M.; Tarver, J. E.; King, B. L.; Newcomb, J. M.; Sempere, L. F.; Flatmark, K.; Hovig, E.; Peterson, K. J. A uniform system for the annotation of human microRNA genes and the evolution of the human microRNAome. *Annu. Rev. Genet.* **2015**, *23*, 213–242.
- [39] Ludwig, N.; Leidinger, P.; Becker, K.; Backes, C. Fehlmann, T.; Palleasch, C.; Rheinheimer, S.; Meder, B.; Stähler, C.; Meese, E.; Keller, A. Distribution of miRNA expression across human tissues. *Nucl. Acids Res.* **2016**, *44*, 3865–3877.
- [40] Girard, M.; Jacquemin, E.; Munnich, A.; Lyonnet, S.; Henrion-Caude, A. miR-122, a paradigm for the role of microRNAs in the liver. *J. Hepatology* **2008**, *48*, 648–656.
- [41] Hu, J.; Xu, Y.; Hao, J. Wang, S.; Li, C.; Meng S. MiR-122 in hepatic function and liver diseases. *Protein & Cell* **2012**, *3*, 364–371.
- [42] He, Y.; Cai, Y.; Paili, P. M.; Ren, X.; Xia, Z. The Causes and Consequences of miR-503 Dysregulation and Its Impact on Cardiovascular Disease and Cancer. *Front. Pharmacol.* **2021**, *12*, 629611.
- [43] Planat, M.; Chester, D.; Amaral, M.; Irwin K. Fricke topological qubits. *Quant. Rep.* **2022**, *4*, 523–532.
- [44] Planat, M.; Amaral, M. M.; Chester, D.; Irwin, K. $SL(2, \mathbb{C})$ scheme processing of singularities in quantum computing and genetics. *Axioms* **2023**, *12*, 233.
- [45] Mir-132. Available online: <https://fr.wikipedia.org/wiki/Micro-ARN.7> (accessed on 1 June 2023).
- [46] Sonkoly, E.; Stahle, M. Pivarsci, A. MicroRNAs and immunity: novel players in the regulation of normal immune function and inflammation. *Sem. in Cancer Biol.* **2008**, *18*, 131–140.
- [47] Micro-ARN 7. Available online: <https://en.wikipedia.org/wiki/MiR-132> (accessed on 1 June 2023).

- [48] Deng, X.; Chen K.; Luo, G. Z.; Weng, X.; Ji, Q.; Zhou, T. He, C. Widespread occurrence of N6-methyladenosine in bacterial mRNA. *Nucl. Acids Res.* **2015**, *43*, 6557-6567.
- [49] Gao, R.; Shi, H.; Zhang, Y.; Shao, X.; Deng, X. N6-methyladenosine modification in bacterial mRNA. *Clin. Microbiol.* **2016**, *5*, 1000256.
- [50] Liu, C.; Cao, J.; Zhang, H.; Yin, J. Evolutionary history of RNA modifications at N6-adenosine originating from the R-M System in eukaryotes and prokaryotes. *Biology* **2022**, *11*, 214.